Holographic Optics for Thin and Lightweight Virtual Reality

ANDREW MAIMONE, Facebook Reality Labs
JUNREN WANG, Facebook Reality Labs

Fig. 1. *Left:* Photo of full color holographic display in benchtop form factor. *Center:* Prototype VR display in sunglasses-like form factor with display thickness of 8.9 mm. Driving electronics and light sources are external. *Right:* Photo of content displayed on prototype in center image. Car scenes by komba/Shutterstock.

We present a class of display designs combining holographic optics, directional backlighting, laser illumination, and polarization-based optical folding to achieve thin, lightweight, and high performance near-eye displays for virtual reality. Several design alternatives are proposed, compared, and experimentally validated as prototypes. Using only thin, flat films as optical components, we demonstrate VR displays with thicknesses of less than 9 mm, fields of view of over 90° horizontally, and form factors approaching sunglasses. In a benchtop form factor, we also demonstrate a full color display using wavelength-multiplexed holographic lenses that uses laser illumination to provide a large gamut and highly saturated color. We show experimentally that our designs support resolutions expected of modern VR headsets and can scale to human visual acuity limits. Current limitations are identified, and we discuss challenges to obtain full practicality.

CCS Concepts: • **Computing methodologies** → **Virtual reality**.

Additional Key Words and Phrases: near-eye display, holography

ACM Reference Format:
Andrew Maimone and Junren Wang. 2020. Holographic Optics for Thin and Lightweight Virtual Reality. *ACM Trans. Graph.* 39, 4, Article 67 (July 2020), 14 pages. https://doi.org/10.1145/3386569.3392416

1 INTRODUCTION

As virtual reality (VR) becomes more ubiquitous, we expect that it will expand beyond entertainment to see broader use in productivity and social interactivity, and these fields will drive VR displays towards more comfortable form factors, higher performance, and improved aesthetics. For example, a VR display used as an immersive computing platform for work would be expected to be used many hours at a time, necessitating a comfortable and lightweight headset. Such a display would also be expected to meet or exceed the performance of conventional displays, and reproduce, for example, small text near the limit of human visual acuity. This use case also brings VR out of the home and in to work and public spaces where socially acceptable sunglasses and eyeglasses form factors prevail.

VR has made good progress in the past few years, and entirely self-contained head-worn systems are now commercially available. However, current headsets still have box-like form factors and provide only a fraction of the resolution of the human eye. Emerging optical design techniques, such as polarization-based optical folding, or "pancake" optics, promise to improve performance while reducing size. However, current implementations rely on curved optics of solid glass or plastic, which has limited designs to goggles-like form factors. In contrast, holographic optical elements can provide arbitrary deflection of light from a flat surface of negligible thickness. However, such elements are difficult to work with due to the need for coherent light sources, wavelength and angle sensitivities, speckle artifacts, and the difficulty of making a full color display.

In this work, we propose combining polarization-based optical folding and holographic optics to gain the performance benefits of both while systematically working through the unique challenges of holography. In particular, we augment these technologies with laser illumination, directional backlighting, and color-multiplexing to achieve the field of view (FOV) and resolution expected of modern VR headsets while reducing thicknesses to ≤ 10 mm to enable sunglasses-like form factors. We demonstrate that our designs scale in resolution to the limits to normal human vision and can exceed the color performance of conventional displays. We propose several design alternatives that are verified in a series of hardware prototypes and discuss challenges to make them fully practical.

1.1 Contributions

We propose designs for near-eye displays that are evaluated across a series of hardware prototypes. Specific contributions include:

(1) We propose a class of near-eye displays combining laser illumination, directional backlighting, color-multiplexed holographic optics, and polarization-based optical folding that is thinner than previously reported VR displays while achieving the resolution and FOV of a modern VR headset.

Authors' addresses: Andrew Maimone, andrew.maimone@fb.com;
Junren Wang, junren@fb.com, Facebook Reality Labs, Redmond, WA, USA.

0730-0301/2020/7-ART67
https://doi.org/10.1145/3386569.3392416

(2) We present several practical and promising design alternatives in the proposed display space that use available and emerging components.
(3) We establish practical means to fabricate full color holographic lenses with sufficient optical power and angular selectivity to be used in the proposed designs.
(4) We evaluate the design through several hardware prototypes and demonstrate beyond state of the art performance in form factor and resolution.

We also identify design limitations and discuss future work necessary to realize full practicality.

2 RELATED WORK

Our proposed design is related to a body of related work in near-eye displays and optics which is summarized below.

Near-eye displays using conventional optics. Near-eye displays for virtual reality using curved reflective and refractive optics have been an area of active research for over 50 years. Common approaches in modern VR headsets include smooth refractive optics, Fresnel refractive optics, and reflective optics incorporating polarization-based optical folding. Geng et al. [2018] provide a recent comparison of these methods. Among these methods, polarization-based optical folding (or "pancake" optics) is recognized as one of the most promising approaches for near-eye display due to the compact size and high performance possible. The method was originally proposed over 50 years ago but has gained momentum with the advent of improved polarization optics, like wire grid [Huxford 2004] and polymeric [Wong et al. 2017] reflective polarizers.

Our proposed method takes advantage of pancake optics to reduce size; however, unlike prior near-eye displays, we use thin and flat holographic films to focus the image, rather than conventional curved reflective and refractive optics. Pancake optics incorporating holograms have been proposed for use in flight simulators by LaRussa and Gill [1978], but to our knowledge have not been applied to near-eye display. Building on this early work, we describe how to adapt holographic pancake optics to near-eye display, systematically working through challenges in lens fabrication, polarization optics, light sources, and display illumination, while minimizing size. We also introduce polarization-sensitive holograms to the design space. Using these optimizations, we demonstrate prototypes with track lengths from the display surface to front optical surface as small as 7.45 mm, or less than half that of recent size-optimized pancake designs [Narasimhan 2018; Wong et al. 2017].

Near-eye light field displays. An alternative method to create a thin virtual reality display is to synthesize a light field near the eye. Lanman and Luebke [2013] show how a microlens array placed over a display panel can create the focal depth cues and has produced the thinnest VR display known to date at 10 mm thick. With further engineering, designs could also likely be made significantly thinner. Although highly innovative, the display sacrifices significant spatial resolution to generate the light field, and published prototypes [Huang and Hua 2018; Lanman and Luebke 2013] have preserved <10% of the resolution of the underlying display panel. The theoretical maximum resolution of the display is also limited by the aperture diffraction of the microlenses. An alternative design, Pinlight Displays [Maimone et al. 2014], creates an image without lenses using a structured backlight consisting of point light sources. The design preserves much of the resolution of the underlying display panel, but has a very low diffraction limited resolution. In contrast to these light field designs, the proposed design is capable of preserving the full resolution of the display panel and has been demonstrated in slightly thinner form factors. Our optical design does not have a practical diffraction limit on resolution and we demonstrate that it scales to the limit of normal human vision. However, unlike light field displays, we will require additional hardware to support the focal depth cues as discussed in Section 6.1.

Holographic near-eye displays. Holographic optical elements (HOEs) have been proposed in near-eye display to replace conventional optical elements, like refractive lenses and prisms. For example, Aye et al. [2001] demonstrate the use of transmissive HOEs to create a near-eye display in a simple magnifier configuration, and Ando et al. [1998] use an HOE as a see through optical combiner. See Kim et al. [2017] for a recent survey of holographic optical elements. Like these past works, we use HOEs as a tool for near-eye display, but in a unique family of optical designs.

Pupil replicating waveguide displays (e.g. Draper et al. [2019]), in which the rays from a small projector are injected into a waveguide and replicated to expand the viewing eye box (i.e. the region in which the eye can see the image), typically use holographic or diffractive gratings as the waveguide in- and out-coupling elements. These designs are one of the leading candidates for augmented reality display due their very compact form factors; waveguide displays are typically only a few millimeters thick, excluding projector optics. However, typical horizontal fields of view of commercial headsets (e.g. Microsoft HoloLens 2, Magic Leap One) are around 40°, limiting their potential use for virtual reality. Further expanding field of view in waveguide displays is challenging due to the limited range of angles that can be carried by total internal reflection in the waveguide. While not as thin as waveguide-based approaches, our proposed design supports the field of view of modern VR headsets ($\geq 90°$) in form factors approaching sunglasses.

Dynamic holographic displays, in which the image itself is formed holographically, have also been proposed for virtual and augmented reality. A recent example by Maimone et al. [2017] shows an augmented reality display in a sunglasses-like form factor. However, dynamic holographic displays have a limited product of display area and light emission angle (or étendue) that is determined by the number of pixels on their light modulators. Current wide field of view dynamic holographic displays typically have a viewing eye box of 1 mm or less, limiting their practicality, and are also very computationally expensive. Techniques such as tracking the eye and dynamically moving around the eye box [Jang et al. 2018], or pupil steering, show some promise of alleviating this limitation, but have not yet been demonstrated to be practical. In contrast, our proposed approach does not have a significant theoretical limitation on eye box. However, the size of the eye boxes in our prototype displays must be modestly increased to enable practical stereo display.

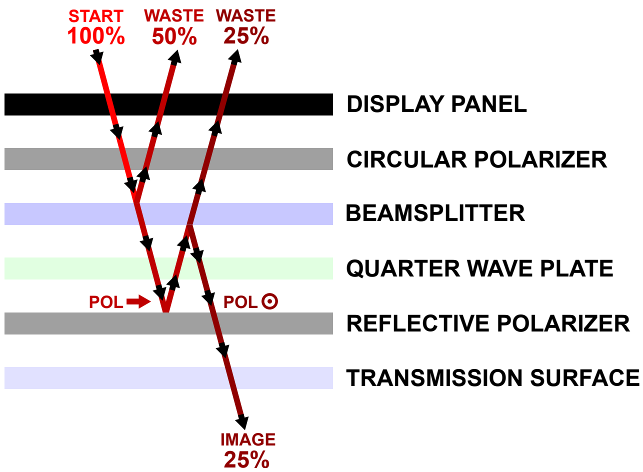

Fig. 2. Pancake Optics. Polarization-based optical folding, or "pancake" optics, allow the cavity between a beamsplitter and reflective polarizer to be traversed three times, which reduces space and improves performance. The polarization state of light is used to control when light exits the cavity.

3 SYSTEM OVERVIEW

The goal of our work is to create a near-eye imaging system that focuses light from a display panel to a distant plane that is within the accommodation range of the viewer. If we assume that the distant plane is at optical infinity, then the job of the display optics is to transform the light emitted from each point on the display panel to a parallel (i.e. collimated) bundle or rays that covers a viewing eye box near the viewer's eye. In doing so, we aim to support a large field of view ($> 90°$) and high resolution that ideally matches the acuity of normal human vision ($\frac{1}{60}^{\circ}$ or 1 arc minute). The display should also be as thin and light as possible and provide a sufficiently large viewing eyebox (> 10 mm) to support eye rotation.

3.1 Proposed Approach

Generally, the constraints listed at the beginning of Section 3 are in conflict. For example, one of the key factors that determines display performance is the *focal length* of the optics, which is related to the distance between the display panel and the focusing optics. Longer distances increase performance, but tend to increase the size of the overall display system.

Polarization-based optical folding (or "pancake" optics) is a design strategy for near-eye display design that effectively increases the distance between the display panel and focusing optic without increasing physical size. The basic concept of pancake optics is shown in Figure 2. A cavity is created between a beamsplitter surface (nominally reflecting 50% and transmitting 50% of incident light) and a reflective polarizer that reflects light from one linear polarization and transmits the orthogonal polarization. A quarter wave plate is placed inside the cavity so that light changes from one linear polarization to the orthogonal polarization between the first and second interaction with the reflective polarizer surface. The light incident on the cavity is in the correct circular polarization state such that that light will be reflected on the first interaction with the reflective polarizer and transmitted on the second interaction.

The primary advantage of pancake optics is that light traverses the length of the cavity three times while only occupying the physical space of one cavity length. This allows the focusing optics to be placed physically close to the display panel, while virtually acting as if they were much further away, providing a tremendous advantage in compactness. There are two major limitations of pancake optics, however. First, light interacts with the beamsplitter surface twice and loses half the light each time, so the overall light efficiency is at most 25%. Secondly, perfect control of light polarization is necessary to ensure that light takes the intended path through the pancake cavity. In practice, pancake designs tend to have some leakage from incorrect polarization, causing faint, out-of-focus copies of the image at different magnifications, also known as "ghost" images.

In a conventional pancake design for near-eye display, focusing power is added by some combination of curving the reflective beamsplitter surface, curving the reflective polarizer surface, or by adding refractive transmissive surfaces. From a size and weight standpoint, this approach has two main disadvantages. First, the focusing power of the surfaces is limited by their physical curvature, which limits the minimum size. Second, refractive surfaces add significant weight to the display, and it is common for the entire pancake cavity to be filled with glass or plastic [Wong et al. 2017].

Our proposed approach is to design a pancake optic where all the focusing power is performed by holographic optical elements rather than bulk optics. Holographic films can replace the reflective beamsplitter surface, the reflective polarizer surface, or both. We can also add transmissive holographic surfaces throughout the design. These are several advantages to this approach. First, all the active optical elements in the viewing optics consist of thin, flat films of negligible weight; most weight comes from supporting substrates, which can be as thin as is mechanically acceptable. The result is very lightweight optics as most of the volume is just air. The flat holographic surfaces can have also arbitrarily high focusing power, subject only to optical aberrations and practical fabrication constraints, which allows the design to be made as thin as possible. Finally, holographic lenses can be constructed so that the lens profiles can be independently controlled for each of the three color primaries, giving more degrees of freedom than refractive designs. When used with the requisite laser illumination, the displays also have a very large color gamut.

Although conceptually simple, there are several challenges to realizing this family of designs. First, holographic optics only work over a limited range of angles and wavelengths, which necessitates a set of careful design considerations. The limited angle range of the elements also compels the design of *directional* backlights in which the emission cones vary spatially over the display panel. The highly dispersive nature of holographic elements also drives the need for laser illumination, which requires a separate source for each color and has challenges in eliminating speckle. Finally, polarization-sensitive volume holograms [Kobashi et al. 2016; Lee et al. 2017], which would comprise the reflective polarizer surface, are an emerging technology and require development for use in our application.

3.2 Components

To apply holographic optics to a near-eye display with polarization-based optical folding, we must reevaluate most of the system components. In this section, we discuss considerations affecting each display component and provide recommendations.

3.2.1 Light Source and Display Panel. Holographic lenses are much more *dispersive* than ordinary refractive lenses, i.e. they bend light at significantly varying angles depending on wavelength. This presents a challenge for a color display because only one color channel will be substantially in focus, which we handle by recording three wavelength-selective holographic lenses as described in Section 3.2.2. However, within a color channel, we must also ensure that the spectrum is sufficiently narrow so that the resolution is not compromised. This effect can be estimated using the diffraction equation:

$$d(\sin\theta_1 + \sin\theta_2) = \lambda \tag{1}$$

where the pitch of the fringes d at a point on a holographic lens is computed from the recording angles θ_1 and θ_2 and recording wavelength λ. When operating the lens, we can use this computed pitch d and substitute θ_1 and λ for the incident angle of light on the lens and playback wavelength respectively to compute the output angle θ_2. By varying λ, one can determine how much angle of the light θ_2 changes over wavelength. From Equation 1, we observe that holographic lenses become more dispersive as the fringe pitch decreases, which generally increases with the radial distance from the lens center. Thus, increasing the spectrum of the source will limit the maximum resolution of the display, with more resolution lost away from the center of the FOV. Within the space of displays considered in this work, a spectral bandwidth of 0.1 nm to 1 nm is generally needed for best performance. This spectrum is far narrower than that of ordinary displays, e.g. an LED-backlit LCD panel or an OLED panel, but can be achieved using a laser illuminated LCD. An advantage of laser illumination is that the narrow spectrum allows a large color gamut and very saturated colors to be produced. The laser sources may also be coupled into an optical fiber, which gives flexibility in their placement, including off the headset.

A side-effect of using a light source with a narrow spectrum, or high *temporal coherence*, is speckle [Goodman 1976], or pseudo-random high spatial frequency intensity patterns in the image that are the result of constructive and destructive interference from rough and structured surfaces on the optics. One solution is to reduce the *spatial coherence* of the source; this is often accomplished by adding a diffusing element with a time varying pattern. One attractive solution is an electroactive polymer diffuser [Blum et al. 2012], which is non-mechanical, compact, and can change diffuser patterns at rates above the human flicker fusion threshold.

3.2.2 Beamsplitter Optic. The beamsplitter surface is one of the two reflective surfaces in the pancake design. If this surface has no focusing power, it can be implemented using a 50% reflective flat mirror. If the surface requires focusing power, it can be implemented as a partially reflective hologram. The surface is a good candidate for adding focusing power because it is farther away from the display panel than the other reflective surface (i.e. the reflective polarizer surface), after unfolding the pancake cavity. This allows a longer focal length focusing element to be used.

To add focusing power to the beamsplitter surface, a volume holographic optical element will be used. A *volume* hologram has a 3D structure that makes the element sensitive to the angle and wavelength of the incident beam; we require wavelength selectivity to handle full color holograms. The HOE modifies the phase of the incoming wavefront by applying a small modulation of the index of refraction throughout the material's volume. (See Goodman [2005] for an introduction to volume holography.) On the beamsplitter surface we record holograms that reflect and focus light much like a concave mirror, but from a flat surface. To record the reflection holograms, we create an intensity pattern over the hologram material by interfering two mutually coherent laser beams. The period of the pattern at a point on the hologram satisfies Equation 1. During playback, the reflected angle of an arbitrary incident ray can be computed by substituting the angles into the equation. Specific element profiles will be discussed in Section 3.3, and their recording configuration in Section 4.1.

A challenge of using volume holographic optical elements for a virtual reality display is their inherent angular selectivity. Unlike conventional reflective and refractive optics, which operate at any incident angle, a volume hologram has an effect over a limited range of angles, typically a few degrees to a few tens of degrees. Another related challenge of volume holograms is that they only have an effect on a portion of the incident light, while some of the light passes through as if the hologram were not present. The fraction of incident light that is affected by the hologram is known as the *diffraction efficiency* (or *efficiency*) of the element. Calculating the efficiency of a volume hologram, given material properties and recording and playback geometries, is complex topic that is out of scope of this paper; Kogelnik [1969] provides a commonly used approximate calculation method.

In the selection of volume hologram recording materials and geometries we have several considerations. The hologram should be sufficiently wavelength-selective so that it affects only one of the color primaries. Ideally, the HOE should also have the target efficiency (50% for the beamsplitter surface) for every ray that passes through the display given the designed FOV and eye box. If the hologram is too angular selective, parts of the FOV or eye box may be dim or disappear. To achieve full color holographic elements, we must record three independent holograms, each of which responds to one wavelength. The holograms can be recorded in a shared volume or in separate layers. Holograms recorded in separate layers tend to have higher efficiency but require careful alignment.

3.2.3 Directional Backlight. A typical display panel emits light in all directions, approaching 180° over of the plane of the display. In a typical near-eye display, only a fraction of this light contributes to the viewing eye box of the display, and the rest is wasted. Additionally, the wasted light can scatter inside the display and cause a reduction of image contrast. Beyond these limitations, holographic optics present an extra challenge because of their limited angular selectivity. A large portion of the light from the display panel will pass through the holographic optics unaffected and can contribute to "ghost" images and a further reduction in contrast if there is leakage through the polarization optics.

To reduce these effects, we apply a technique called *directional backlighting* in which the emission angles of the display panel are controlled. This technique has been employed to improve the light efficiency of a display [Wang et al. 2015]. In our case, we must design a backlight that emits only (or approximately) the light rays that are carried through through the optical system to the viewing eye box to prevent excess leakage. Depending on the optical design, the required emission pattern may be a simple uniform pattern, i.e. a limited range of angles relative to the display normal, or a spatially varying pattern over the display panel. We consider both cases in the designs proposed in Section 3.3.

We investigated two options for directional backlights. The first is *light shaping*: we fabricate an element that transforms the light source into the wavefront required by the backlight. The light shaping approach can be implemented as an additional holographic element that is recorded using two beams: one that matches the emission distribution of the light source (e.g. a point source) and one that matches the desired emission profile of the directional backlight. To keep the backlight compact, the source may be coupled into a thin waveguide that carries light from the source by total internal reflection until it is out-coupled by the holographic element. The advantage of this approach is light efficiency. Theoretically, most all of the light from the source can reach the viewing eye box; however, it may be difficult to fabricate a high efficiency holographic directional backlight in full color and in challenging compact geometries. The second option considered is a *light-attenuating* directional backlight, in which we start with rays emitted in all directions (i.e. a conventional backlight) and cull them to the subset that contributes to the viewing eye box. This can be achieved geometrically with a louver-like structure, e.g. a plate consisting of bundles of opaque and transparent optical fibers. Such plates are available commercially (Incom DARC Glass) in thin form factors of ≤ 1 mm. Although the light attenuating approach is less efficient, it can be implemented readily on top of conventional display backlights.

3.2.4 Reflective Polarizer Optic. The reflective polarizer is the second of two reflective surfaces in the pancake design, and controls when light exits the cavity. If the surface has no focusing power, it can be implemented with various technologies such as wire grid or polymeric films. If the surface has focusing power it can augment the beamsplitter surface and provide additional degrees of freedom. In pancake designs using conventional optics, reflective polarizers using curved polymeric films have been demonstrated [Wong et al. 2017]. However, we cannot directly apply ordinary volume holograms to this surface since they are not polarization sensitive.

Polarization-sensitive volume holograms (PVH) are an emerging technology with practical examples appearing in just the past few years [Kobashi et al. 2016; Lee et al. 2017]. These are a fundamentally different technology than conventional volume holograms and consist of thin polymerizable liquid crystal materials. Like traditional volume holograms, PVHs exhibit some wavelength and angle sensitivity and can potentially be stacked to make a full color element. Note that the polarization sensitive holograms that we consider in this work (see Section 4.1.2) reflect one circular (rather than linear)

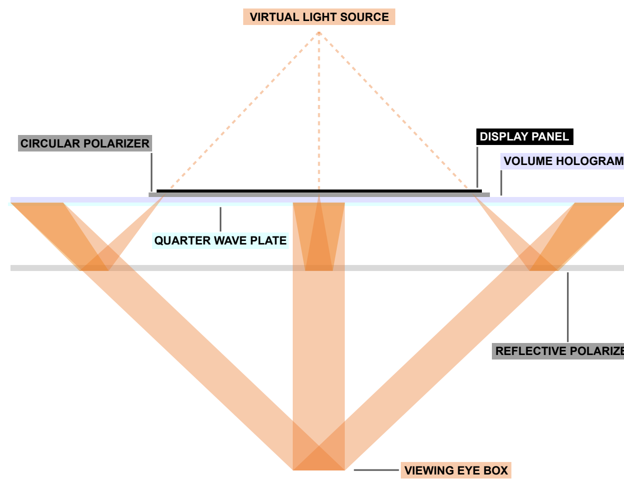

Fig. 3. Optical design using one reflective surface. Polarization-based optical folding is used in a configuration with all of the focusing power on the holographic beamsplitter surface.

polarization and transmit the other, and the reflected beam maintains the same polarization as the incident beam. Thus, if we replace the reflective polarizer with a polarization volume hologram, we can remove the quarter wave plate from the pancake cavity.

3.2.5 Transmissive Optics. As with a conventional pancake designs, we can also add transmissive surfaces to the design. However, a major challenge of using transmission holograms is diffraction efficiency. Unlike reflection holograms on the beamsplitter surface, the light that is not diffracted by a transmission hologram in our design will ultimately propagate toward the eye and could result in strong ghost images or contrast loss. Thus we would like transmission holograms to have very high efficiency (ideally 100%) over a large angle range, which is difficult to achieve with volume holograms today. One potential solution is a multi-stage lens designed to direct transmission leakage away from the eye [Aye et al. 2001].

3.3 Optical designs

In this section, we will propose some specific optical designs using the component toolset described in Section 3.2, while considering trade-offs in performance and complexity.

3.3.1 One reflective surface design. For an initial optical design, we seek to build a display that can be assembled with off-the-shelf or easily constructed parts and that provides reasonable performance. First, we must determine which surfaces to apply holograms and focusing power. Since the components needed for the reflective polarizer surface require emerging technologies (see Section 3.2.4), we elect to place all focusing power on the beamsplitter surface.

Next, we must determine where to position the beamsplitter surface and the holographic lens profile to add to that surface. In doing so, we make a few considerations:

(1) To make the hologram simple to construct with off the shelf optics, the recording beams should be converging or diverging point sources. Since the designs are expected to be radially

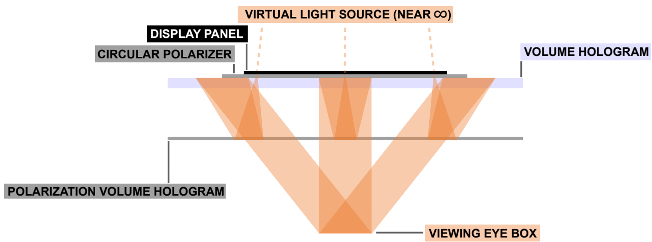

Fig. 4. Optical design using two reflective surfaces. Polarization-based optical folding is used in a configuration where the focusing power is shared between holograms on the beamsplitter and reflective polarizer surfaces.

symmetric, the lens will be defined simply by the distances of the sources from the recording film along the optical axis.

(2) The beams used for recording and playback should be similar so that the hologram has high efficiency during playback.
(3) The holographic lens should have sufficiently broad angular selectivity with off the shelf recording materials to support an eye box large enough for a monoscopic display prototype.
(4) The wavefront emitted by the required directional backlight should be reproducible with easily constructed parts.
(5) The display should provide a FOV and resolution comparable to modern VR headsets in a thin form factor, e.g. $\leq$ 10 mm.

While considering these constraints, we observed that a hologram designed to focus light from a point source at distance d from the recording media back onto itself is a particularly attractive solution. A reflection volume hologram tends to have broad angular selectivity when used with a beam that is at normal incidence to the holographic fringes in the material. In the proposed *retroreflective* configuration, this criteria is approximately met everywhere on the holographic lens, so angular selectivity is broad and uniform. When such a lens is optimized for best performance with polarization-based folding, the playback angles roughly match the recording angles, which maximizes diffraction efficiency. The required directional backlight is a virtual point source behind the display, which is feasible to reproduce. Performance is quite reasonable for a display with a thickness of $\approx$10 mm, which is surprising since it only has a single focusing surface with a single degree of freedom (distance d). Thus, this configuration meets all of our design criteria.

The display design using such a hologram is illustrated in Figure 3. To maximize performance, we put the beamsplitter surface adjacent to the display panel to maximize its unfolded distance to the panel. An ordinary (unpowered) reflective polarizer is used and there are no transmissive holographic elements. A backlight reproducing a virtual point source can be fabricated as an additional volume hologram behind the display panel, which is demonstated in Section 4.1.3. We prototyped two displays using this optical design, which are described in Sections 4.2.1 and 4.2.2.

3.3.2 Two reflective surfaces design. Although the one surface reflective design described in Section 3.3.1 is a good initial starting point, it has a few limitations:

(1) Optical performance could be improved. To scale our design to higher resolutions (approaching human acuity limits), we will likely need more degrees of freedom in our optical design.
(2) The required directional backlight creates a virtual point source that is placed at a close distance behind the display panel. Light rays emitted from the backlight will fan out significantly before they are focused by the holographic beamsplitter surface. This creates large regions of the display that do not contribute to the display's FOV or viewing eye box, so the display may be laterally quite large (although thin).
(3) Although the directional backlight is practical to fabricate, there are more fabrication options for directional backlights that do not have spatially varying emission patterns.

To address these limitations, a straightforward direction is to gain degrees of freedom by adding focusing power to the reflective polarizer surface in addition to the beamsplitter surface. In doing so, we'll consider a few constraints. First, the hologram on the beamsplitter surface already provides near optimal selectivity and efficiency characteristics so we prefer not to change it significantly when adding the powered reflective polarizer surface. To avoid the fan out region in the display and the need for a spatially varying directional backlight, the central rays emitted from each pixel on the display panel should be substantially collimated. Finally, since polarization volume holograms can be fabricated by programmable exposure of a photoalignment layer [Kobashi et al. 2016], it is possible to generate surfaces with higher degrees of freedom.

Taking these constraints into account, we designed an aspheric polarization volume hologram that meets our design goals. The element accepts light from a backlight where the central rays emitted from each pixel are substantially collimated and bends it towards the angles required for the retroreflective hologram on the beamsplitter surface (see Figure 4). The element also corrects some of the aberrations present on the beamsplitter surface to achieve significantly higher performance. The phase profile for the optimized reflective polarizer hologram can be described as a radially-symmetric polynomial. A backlight suitable for use in this design can be constructed by injecting laser light into an ordinary LCD backlight module, and placing an angle-restricting plate on top. We prototyped a display using this optical design which is described in Section 4.2.3.

3.3.3 One transmissive surface design. Although the design in Section 3.3.2 has attractive performance, display designs featuring transmissive holographic surfaces can offer even better performance. The reason is intuitive: after unfolding, the transmission surface is three pancake cavity lengths away from the display, while the beamsplitter surface is two and the reflective polarizer is only one. Thus, we can use a much longer focal length holographic lens on the transmissive surfaces than the other surfaces while retaining the same thickness. In fact, excellent performance is possible by placing all the focusing power on the transmissive surface, in which case the beamsplitter and reflective polarizers are unpowered surfaces that just collapse the space between the panel and transmissive lens (see Figure 5). Further, excellent performance can also be achieved with a transmissive lens having a simple phase profile that can be described as a quadratic function. Such a lens also requires a backlight where

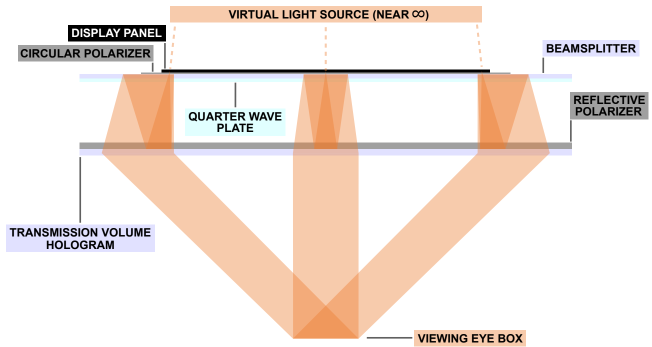

Fig. 5. Optical design using one transmissive surface. Polarization-based optical folding is used in a configuration where all of the focusing power is on a transmission hologram placed after the pancake cavity.

the central rays emitted from each pixel are substantially collimated, which is convenient to fabricate.

Although this design offers the best theoretical performance, it is difficult to realize due to the leakage of transmissive holographic optical elements available today. For this reason, we did not construct a prototype in this design but rather relegate as a promising potential path for future work as transmissive holographic optical elements continue to improve.

4 IMPLEMENTATION

We constructed three prototype displays to evaluate various aspects of our display designs. The fabrication of display components is described in Section 4.1, and the integration of the complete display prototypes is described in Section 4.2.

4.1 Component fabrication

4.1.1 Holographic Optical Element Fabrication. We optically recorded volume phase holograms into photopolymer film (Liti Holographics C-RT20) by two beam interference (see Figure 6). For full color holograms, three color holograms were multiplexed into a single film by simultaneous recording with co-aligned red (Cobolt Flamenco 660 nm, 0.5 W), green (Cobolt Samba 532nm, 1.5W), and blue (Coherent Genesis CX 460 nm, 2W) lasers whose power levels were adjusted to give approximately equal diffraction efficiency across colors. The holograms operate in reflection mode and are designed to record a “retroreflector” lens profile that focuses a point light source at a distance d from the lens back onto itself. Among the three prototypes, we constructed lenses where $d = 21$ mm, $d = 26$ mm, or $d = 36$ mm. The profile was recorded using two high numerical aperture aspheric lenses that create diverging and converging beams. The beams share a common focusing point that is at a length d in front of the holographic recording film. The resulting lenses have very high focusing power; the focal length of the lenses is approximately one quarter of the lens diameter. The distance d (and other display parameters) were chosen by numerical optimization to provide the best performance within a target display thickness.

4.1.2 Polarization Volume Hologram Fabrication. We fabricated polarization volume holograms designed to operate in green light at 532 nm. We first wrote the pattern of the desired aspheric lens profile to a photoalignment layer coated on a glass substrate using a custom programmable recording tool. A liquid crystal reactive mesogen (RM) solution was then spin-coated on top of the patterned photoalignment film. Due to self-assembly, the RM layer follows the pattern of the photoalignment layer, creating a volumetric structure. Afterwards, the RM layer was UV cured into a robust polymer film.

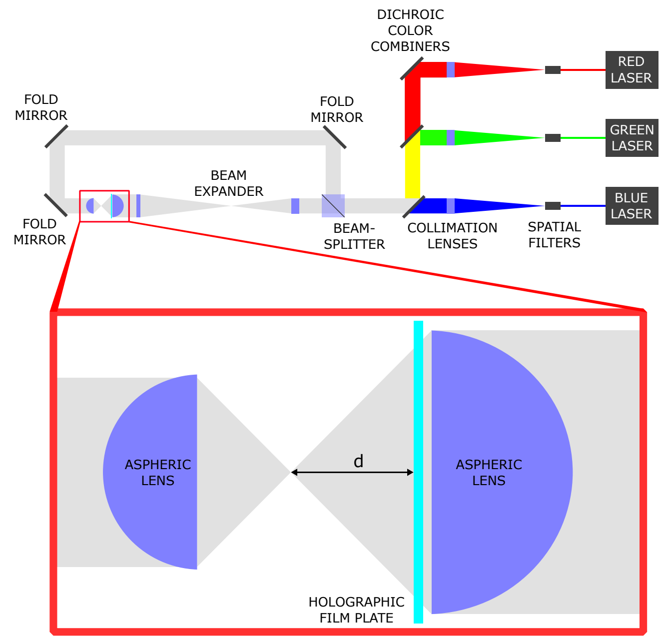

Fig. 6. Holographic optical element recording table layout. Two powerful aspheric lenses are used to record a holographic lens that focuses a point at a distance d from the hologram back onto itself. Three lasers are used for full color recording.

4.1.3 Holographic Directional Backlight Fabrication. A holographic directional backlight was recorded using two beam interference into holographic photopolymer film (see Figure 7) using 532 nm green light. The first recording beam was a diverging point source at the edge of the holographic plate which propagates down the plate through total internal reflection. The second beam was a diverging point source at a distance of 13 mm away from the recording plate. A diffuser was placed between the second point source and the holographic plate to create an extended light source and expand the viewing eye box. The resulting directional backlight shapes the light from a fiber optic cable placed at the edge of the backlight into an extended virtual light source that is 13 mm behind the display.

4.2 Display prototypes

We designed three display prototypes to test various aspects of our display design, such as full color operation, sunglasses-like form factors, and support for high resolution. Each prototype follows one of the designs outlined in Section 3.3 and was modeled in optical design software (Zemax OpticStudio). Specific parameters (lens parameters, component spacing, etc.) were numerically optimized

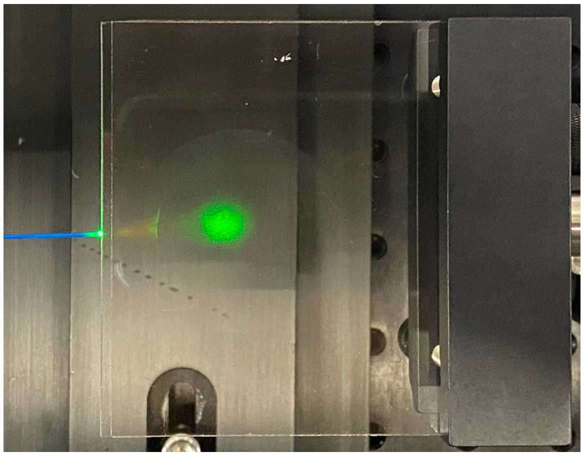

Fig. 7. Holographic directional backlight. Light from an optical fiber (blue component to left) is injected into a 1 mm thick waveguide to form a virtual extended light source at a distance of 13 mm behind the display. The virtual source is formed by a holographic film on the underside of the waveguide.

in the design software with the goal of achieving the best modulation transfer function (MTF) at the maximum spatial frequency supported by the display panel. Optimization was performed over a viewing eye box of 8 mm, which is approximately the size we achieve in our display prototypes with off the shelf recording film.

4.2.1 Benchtop prototype. The goal of the first prototype is to demonstate a thin eyepiece, a wide field of view, and full color dynamic display in a benchtop form factor (see Figure 8). The prototype follows the one reflective surface design described in Section 3.3.1. The display was illuminated with a Cobolt Skyra laser that provides three laser lines (457 nm, 532 nm, and 660 nm) into a shared single mode optical fiber. The relative powers of the lasers were adjusted to balance colors for the display.

The laser light is coupled into a large, unfolded directional backlight that was not integrated into the display. The backlight consists of off-the shelf components held in place with optomechanical mounts. In the backlight, light from the optical fiber passes through a despeckler unit (Optotune electroactive polymer laser speckle reducer) and then an optical diffuser, creating an extended area source at a distance of 20 mm from the display panel. We use a 2.1" 1600×1600 LCD panel to form the image.

The prototype uses a three color holographic element as the beamsplitter surface. The active diameter of the lens is approximately 75 mm and is designed to focus light from a point at a distance $d = 36$ mm away from the lens back onto itself. To build the display, all components except the reflective polarizer were stacked on top of each other and a 3D printed frame was placed on top of the stack to hold the reflective polarizer. The frame maintains an air gap of 7.3 mm between the reflective polarizer and the other components.

The overall size of display, including the 3D printed frame, is 82 mm $\times$ 82 mm. The distance from the display image surface to the last active optical surface (which we call the *imaging track length*) is 9.85 mm. The LCD panel components behind the imaging surface and cover glasses add an additional 1.15 mm, for a total display

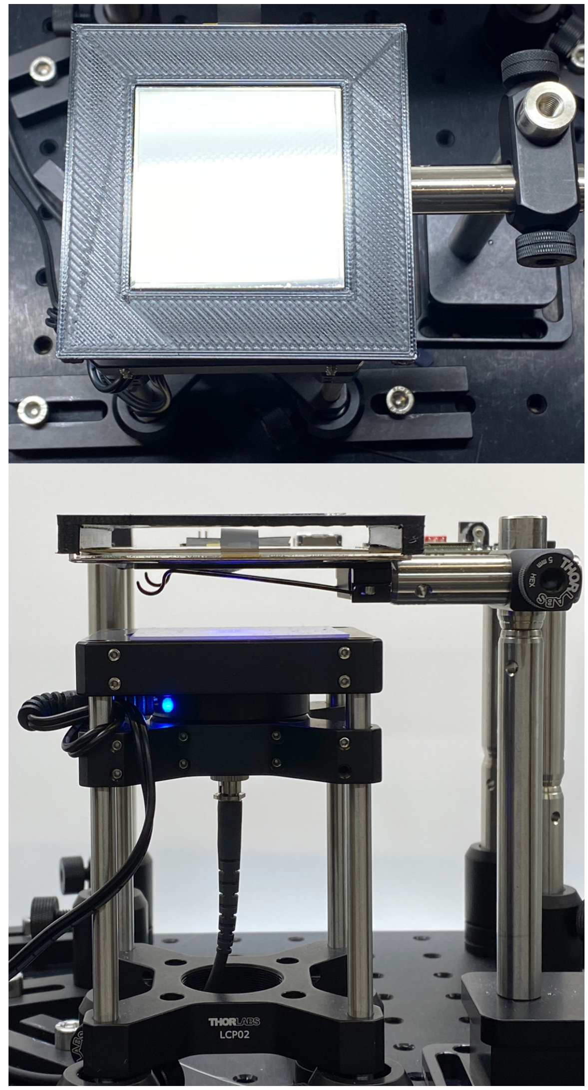

Fig. 8. Benchtop prototype. A full-color display was prototyped in an 11 mm thick optical stack plus an external directional backlight that forms an extended light source at a distance of 20 mm below the display.

thickness of 11 mm, excluding the large backlight unit that was not integrated into the display.

4.2.2 Dynamic sunglasses prototype. The goal of the second prototype is to demonstrate the viability of fitting a complete, wide FOV, dynamic display into a sunglasses-like form factor with a thickness of < 10mm. The prototype follows the one reflective surface design of Section 3.3.1, but is implemented at a smaller scale than the benchtop prototype and has an integrated backlight. For simplicity, the prototype was designed to operate in the green channel only.

The display is illuminated with a Thorlabs DJ532-40 532 nm laser that is de-speckled by an Optotune electroactive polymer speckler reducer and then coupled into a multi-mode fiber. The tip of the fiber is placed at the edge of a waveguided holographic directional

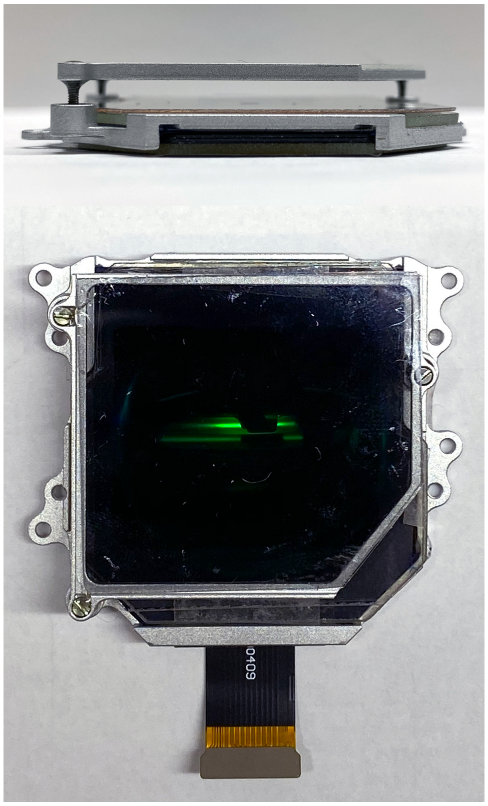

Fig. 9. Display module for dynamic sunglasses-like prototype. A compact display module consists of a backlight, display panel, and eyepiece mounted in an aluminum frame. The total thickness of the module is 8.9 mm. (Note that the green lines seen on the module are an image of the ceiling lamps being focused by the holographic lens.)

Fig. 10. Sunglasses prototype. A sunglasses-like prototype consists of two optical modules mounted in a 3D printed frame. Note that driving electronics and light sources are mounted externally to the glasses.

backlight which creates an extended area source at a distance of 13 mm behind the display. The backlight is integrated into the display and adds approximately 1 mm thickness. A 2.1" 1600 × 1600 LCD panel is used to form the image. However, note that the display panel is larger than is required for the optical design, and thus the image seen by the display is approximately 1000-1200 pixels across.

The prototype uses a single color holographic element as the beamsplitter surface. The lens is designed to focus light from a point at a distance $d = 26$ mm away from the lens back onto itself. To build the display, the optical components are mounted into two custom aluminum frames: one that holds the reflective polarizer, and one that holds all other components. Thin rods are used to maintain an air gap of 5 mm between the two sets of components. The overall size of the complete assembled display module is 53 mm × 48 mm at the widest points (see Figure 9). The imaging track length of the display is 7.45 mm and the full thickness of the module is 8.9 mm, including the display panel and backlight. The weight of the complete module is 17.8 g, including approximately 3 g for the aluminum frames.

The optical module was mounted into a 3D printed sunglasses-like frame, as shown in Figures 1 and 10. Note that only the optical module in the left eye is functional, and that driving board for the LCD panels is housed externally from the glasses and connected with a cable. Light is delivered to the headset via a fiber optic cable, but the laser and despeckler units are also mounted externally.

4.2.3 High resolution static sunglasses prototype. The goal of our third prototype is to demonstrate that our designs can scale to the resolution limits of normal human vision, while maintaining a large FOV and thickness of < 10mm. We also use this prototype as a test vehicle to evaluate emerging polarization volume hologram technology. The prototype follows the two reflective surfaces design described in Section 3.3.2. For simplicity, the prototype is designed to operate in the green channel only.

As with the previous prototype, the display is illuminated with a Thorlabs DJ532-40 532 nm laser that is de-speckled by an Optotune speckle reducer and then coupled into a multi-mode fiber. To form the directional backlight, we started with a backlight that was removed from a 2.1" LCD panel. We replaced the white LEDs in the backlight with the tip of the optical fiber, which was placed against the edge of the backlight's internal lightguide. We placed a 1 mm thick angle limiting fiber optic plate (Incom DARC Glass) over the backlight which limits emission angles to approximately ±12.5° relative to the display normal. Since there are no known display panels with sufficient size and resolution to test our optical design, we elected to use a static mask as a proxy for a display panel. We tested the display with two types of masks: a film photoplot with a minimum feature size of $7\mu m$ and a chrome on glass mask with a minimum feature size of $4\mu m$.

The prototype uses two holographic lenses that have been jointly optimized. The first lens is a hologram on the beamsplitter surface that is designed to focus light from a point at a distance $d = 21$ mm away from the lens back onto itself. The second lens is a polarization volume hologram that comprises the reflective polarizer surface and has an aspheric phase profile that can be described as a fourth degree polynomial. The PVH element is designed to correct some of the optical aberrations of the hologram on the beamsplitter surface.

To build the display, the optical components are mounted into an identical aluminum frame and 3D printed sunglasses frame as the second prototype described in Section 4.2.2 and pictured in Figures 1 and 9, except that the air gap slightly increased to 5.6 mm and the overall thickness is increased 1 mm due to the thicker backlight unit. This prototype is more alignment sensitive than the other prototypes due to the multiple focusing elements and high resolution. Thus, the reflective polarizer frame was actively aligned to the frame holding the other components using a five-axis stage and camera feedback. After alignment, the components were bonded in place and the stage was removed.

The imaging track length of the display is 7.45 mm and the full thickness of the display module is 9.9 mm. The weight of the complete module is 17.3 g, including approximately 3 g for the aluminum frames. Note that the measurements above correspond to the optic module using the film photoplot mask; the version using the chrome on glass mask is slightly thicker (< 1 mm) and heavier. As with the second prototype, only the left eye is populated with a display module and light is delivered to the headset via a fiber optic cable. The laser and despeckler units are mounted externally.

4.3 Results Capture

We used three cameras for system alignment and results capture. An iPhone 11 Pro (ultra wide lens) was used for full color capture of the prototype described in Section 4.2.1 and for field of view estimation. We also used the iPhone 11 Pro's regular wide angle camera to capture color results with a narrower FOV to show more display detail. A FLIR Blackfly S (model BFS-U3-200S6M-C) monochrome camera was used to capture the prototype described in Section 4.2.3 due to the need for very high resolution. The camera has a resolution of 5472 x 3648 and no color filters, so it was able to capture the approximate 5000 display pixels that cover the horizontal field of view of the camera. Note that the monochome image data from this camera is visualized in the green color channel (rather than as gray) to make clear that the captured display is monochrome green. A FLIR Blackfly S (model BFS-U3-200S6C-C) color camera was used to capture the video results for the prototype described in Section 4.2.2. The FLIR cameras were used with a Fujifilm CF8ZA-1S lens with the aperture set between $f/1.8$ and $f/4.0$. Display and camera focus were set close to infinity (< 1 D). Camera images were not post-processed except cropping, rotation, and/or scaling to appropriately present them in the paper.

The prototypes using LCD panels were connected to an external driving board that interfaced with a PC through a DisplayPort link. To show the raw performance of the optics, we directly displayed the source content on the panels and did not provide any software distortion, uniformity, color alignment, or color uniformity correction. However, we expect that doing so would increase performance.

5 EXPERIMENTAL ASSESSMENT

We evaluated our three hardware prototypes by measuring viewing characteristics (FOV, eye box, and eye relief) and the resolution and quality of the produced images. Eye relief was measured from the last optical surface to where the display's exit pupil is formed. All result images were taken at the center of the eye box. Specific results are found in the remainder of this section and results showing dynamic content can be found in the supplemental video.

Fig. 11. Benchtop prototype result. Photograph shows a full color image using three color lasers and color-multiplexed holographic optics. The diameter of the circular FOV shown is 80°. Vegetables image by leonori/Shutterstock.

5.1 Benchtop prototype

For our full-color benchtop prototype, we measured a maximum horizontal field of view of approximately 93° horizontally. Figure 11 shows a photograph of the display having a circular field of view with a diameter of 80°, limited by a round aperture. The viewing eye box is round with a diameter of approximately 8 mm, and falls off in intensity away from the center. The eye relief was measured at approximately 21 mm.

As shown in Figure 11, the display was able to provide vivid, saturated colors (which cannot be fully captured in the image) due to the laser illumination. Speckle was suppressed well by the de-speckler unit. Only a small amount of noise remained, and was most salient during dynamic content. Without the de-speckler unit, the image quality was unacceptably noisy.

The display uses a 1600 × 1600 pixel LCD panel to achieve a resolution of approximately 3.5 arc minutes, which is comparable to or higher than current VR headsets (e.g. Oculus Quest, HTC Vive Pro). Figure 12 (top), shows a magnified region of the scene from Figure 1 (left). In the inset image, one can see the discrete pixel structure of the LCD panel, indicating that the viewing optics can resolve the panel at full resolution.

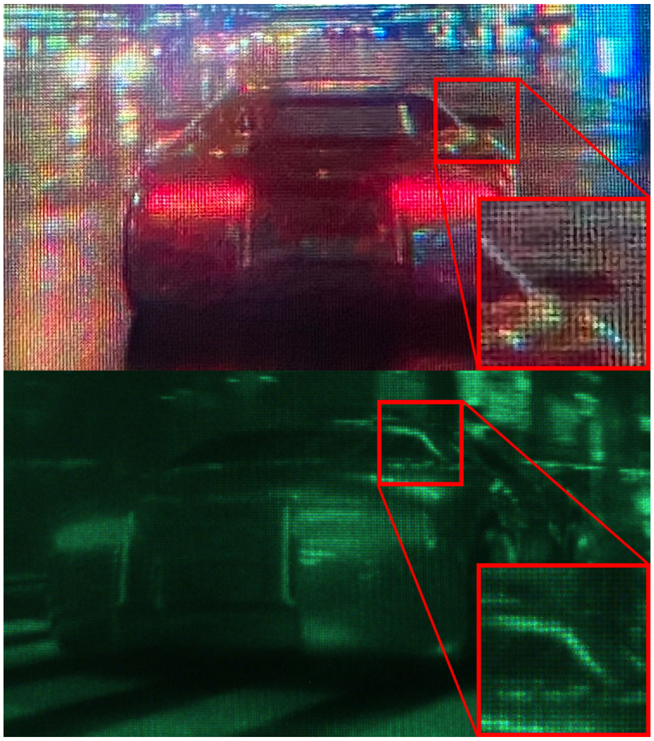

Fig. 12. Resolution of LCD-based prototypes. Photographs show magnified regions of the benchtop (top) and dynamic sunglasses-like display (bottom) using the scenes from Figure 1. The magnified inset images show that the pixel structure of the display is resolved. The top image spans a 12.5° horizontal FOV, while the bottom spans 22.5°. Car scenes by komba/Shutterstock.

Figure 13 shows a photograph of a grid of white lines being displayed. The mostly parallel lines indicate that the display has very low geometric distortion, as predicted in the optical model. However, there are some non-uniformities in the image. The display has some overall vignetting and an uneven spatial color balance; note that the left of the image has a stronger green cast and that the right has a stronger red cast. We expect that we can improve the color balance by ensuring that the hologram recording beams are uniform after spatial filtering. There is also a small misalignment in the color channels that increases radially (see Figure 13 inset), which is likely due to dispersion from the aspheric recording lens. This could be compensated optically by adjusting the plate position for each recording color, or could be compensated more conveniently in software. Finally, note that is there a small blue ghost image of the grid in the center of the field of view due to leakage through the polarization optics. We believe the ghost could be suppressed by ensuring that all surfaces are anti-reflection coated.

5.2 Dynamic glasses prototype

For our green-only sunglasses-like prototype, we measured an overall maximum field of view of approximately $92° \times 69°$; however note there are a few obstructions in the field of view in the peripheral region. Figure 14 shows a photograph of the display which captures

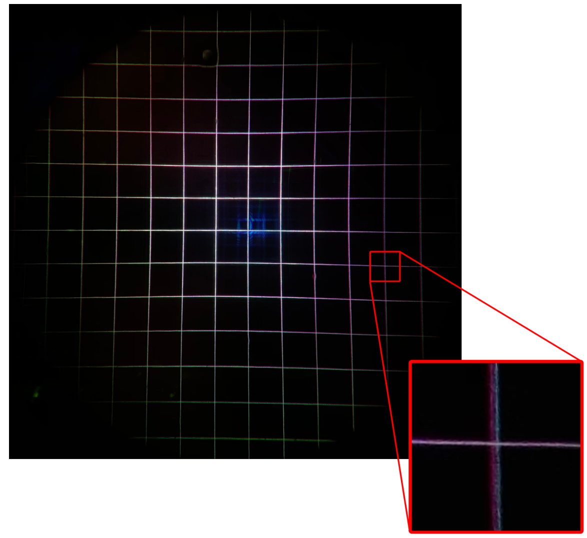

Fig. 13. Benchtop prototype calibration image. Photograph of benchtop prototype displaying a grid of white lines, which reveals color misalignment and non-uniformity issues and a ghost image at the center of the FOV.

$80° \times 67°$ of the field of view. The viewing eye box is round with a radial sinc-like function and a central main lobe of approximately 8 mm. The eye relief was measured at approximately 17 mm.

Figures 1 (right) and 14 show photographs of the display, indicating we are able to produce a high quality image in the sunglasses-like form factor. We note, however, a few artifacts. The image is brighter on the left side of the image due to backlight non-uniformity and there is a bright spot near the fiber tip. Overall, performing the despeckling before injection into the optical fiber was effective, but the image is noisier than the benchtop prototype. This prototype used a de-speckler unit with a smaller diffusing angle, and we expect that we can improve performance by increasing the diffusing angle and using a larger numerical aperture optical fiber. Like the benchtop prototype, geometric distortion is very low. Unlike the benchtop prototype, we do not see a prominent ghost image in the center of the display, likely because more surfaces are anti-reflection coated and there is not substantial leakage in the green channel.

The display uses a 1600×1600 pixel LCD; however, the panel is too large for our optical design and only 1000–1200 pixels are visible. This yields a resolution of approximately 5 arc minutes, which is lower than our benchtop prototype but is comparable to recent commercial headsets (e.g. HTC Vive, Playstation VR). Figure 12 (bottom), shows a magnified region of the scene from Figure 1 (right). In the inset image, one can see the pixel structure of the LCD panel, indicating that the full panel resolution can be resolved.

5.3 High resolution static glasses prototype

For our sunglasses-like prototype featuring a polarization volume hologram, we measured an overall maximum field of view that is round with a 93° diameter; Figure 15 shows a photograph of the display which captures $78° \times 55°$ of the field of view, limited by the lens of our high resolution camera. The viewing eye box is round

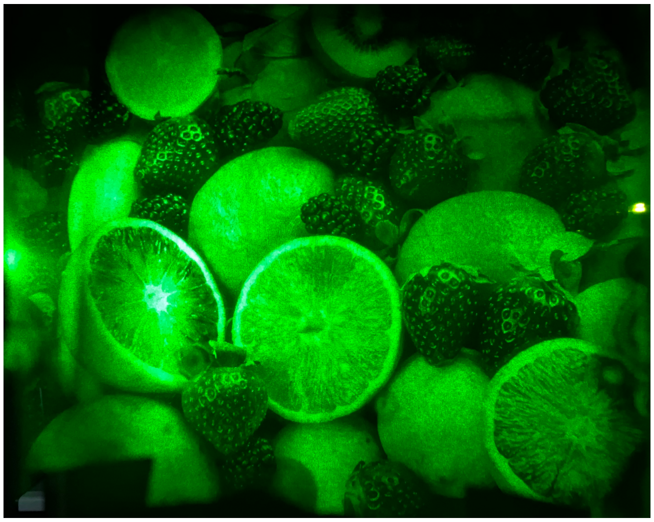

Fig. 14. Dynamic sunglasses prototype result. Photograph shows image being displayed on the dynamic sunglasses-like prototype. The field of view of the image shown spans $80^\circ \times 67^\circ$. Fruits image by leonori/Shutterstock.

with a radial sinc-like function. The first two lobes have strong intensity and span approximately 9 mm; however, there is a thin radial gap in the eye box between the lobes. The gap is smaller than a human pupil diameter so it will not cause a loss of image but may cause dimming in part of the eye box. The eye relief was measured at approximately 14 mm.

Overall, we we able to create a clear, high contrast image in this prototype (see Figure 15); however, there are some notable artifacts. Like the first sunglasses-prototype in Section 5.2, the image is brighter on the side the fiber tip was injected. We expect that this could be improved by better light injection into the backlight that matches that of the original backlight design. There are also some low frequency radial lobes of brightness non-uniformity, which we expect could be improved by more careful writing of the PVH lens profile. There is also some haze in the very center of the display (central +/- 2.5 deg) from the PVH lens, which we expect that could reduced by tuning the writing parameters of the photoalignment mask. As predicted in the simulated model, there is moderate pincushion distortion in the image. However, such distortion is often favored for virtual reality displays since it concentrates resolution in the center of the display, where human visual acuity is the highest. Like the first sunglasses-like prototype in Section 5.2, we do not see a prominent ghost in the center of the image and speckle performance was similar.

We tested the resolution of the display with two versions of the prototype: a medium-high resolution version using a film mask and a high resolution version using a chrome on glass mask. The result using the film mask is shown in Figure 15. The smallest features on the mask, which are a located next to the smaller number *6* in the repeating test chart, are $7\mu m$ lines with a $7\mu m$ space in-between, providing a resolution greater than 2 arc minutes. In the figure, note that even in the corner of the $78^\circ \times 55^\circ$ FOV captured by the camera (see magnified red-bordered inset image) the smallest

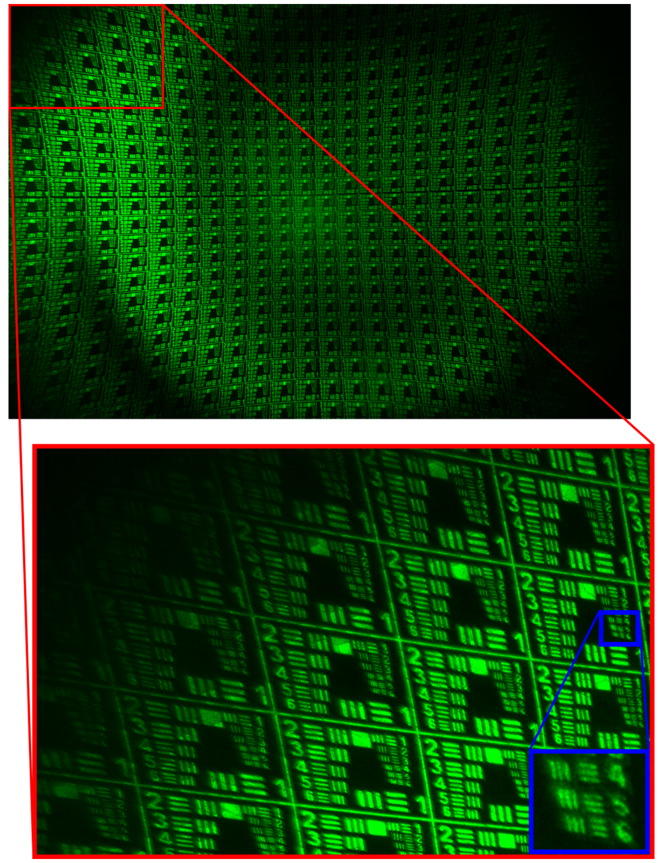

Fig. 15. Photograph of static high resolution sunglasses prototype with film mask. A $78^\circ \times 55^\circ$ FOV was captured by the camera. The red-bordered magnified inset region shows that the display is sharp up to the corners, and the further magnified blue-bordered inset region shows that the smallest $7\mu m$ features are resolved, which have an extent of less than 2 arc minutes.

lines can be resolved (see further magnified blue-bordered inset image). The result using the chrome mask is shown in Figure 16. The smallest features on the mask, which are a located next to the smaller number *6* in the repeating test chart, are $4\mu m$ lines with a $4\mu m$ space in-between. This provides an average resolution greater than 1 arc minute, which is the limit of 6/6 or 20/20 vision. In the figure, we sample multiple positions over the display at different radii from approximately 7.5° to 30° radially from the center of the FOV and show that the smallest features on the chart ($4\mu m$ lines) can just be resolved by the display and camera. Note that the camera and display resolution are approximately matched within the measured area (so that we expect that the minimum features are just resolved), but vary somewhat due to camera and display distortion and are matched at approximately 68 pixels per degree at $\pm 17.5^\circ$ in the field of view. Note that we only tested the central 60° of the field of view using the high resolution mask in Figure 16. Outside this area there was significant ghosting which we expect was caused by an absence of an anti-reflection coating on the thicker chrome on glass mask since the thinner film mask prototype did not exhibit this problem.

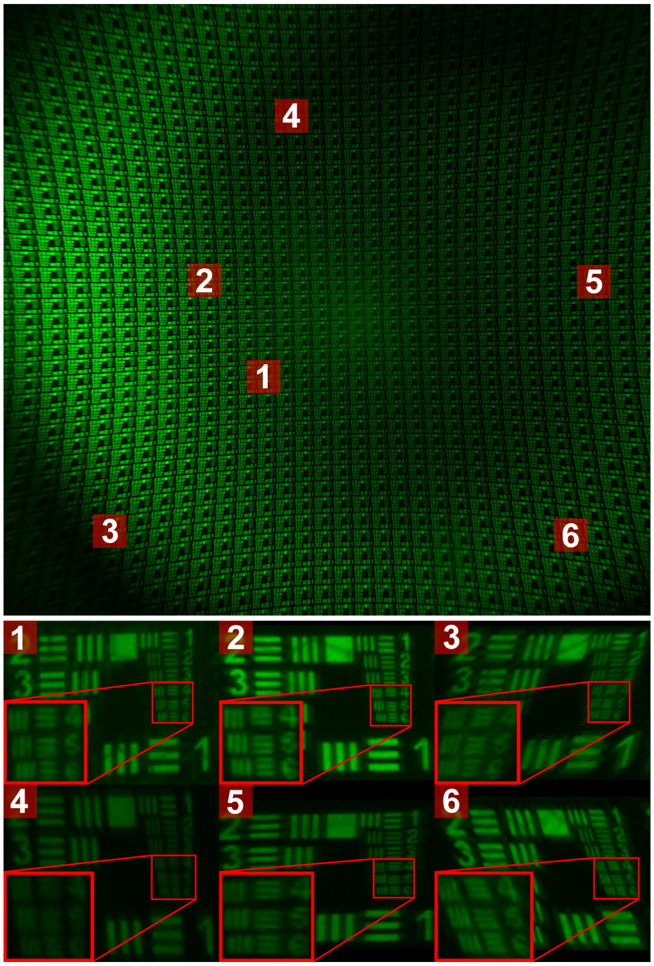

Fig. 16. Photograph of static high resolution sunglasses prototype with chrome mask. Photo shows the central 60° of the FOV. Numbers in top image correspond to locations of magnified regions in bottom images. Note that the display and camera can just resolve the smallest $4\mu m$ features on the mask, which have an extent of approximately 1 arc minute.

6 DISCUSSION

Our experimental results have demonstrated the possibility of wide FOV, high resolution virtual reality displays in the form factor of large sunglasses. We have also demonstrated the viability of full color holographic optics and the ability to scale our designs to the visual acuity limits of normal human vision. However, in the following section, we note several challenges to obtaining full practicality and the best performance.

6.1 Limitations and Future Work

Integrated full color display. We have yet to demonstrate a full color display that is fully integrated into a sunglasses-like form factor. To do so, we must upgrade the prototype described in Section 4.2.2 to support a full color holographic directional backlight, or we must construct a full color polarization volume hologram lens for the prototype described in Section 4.2.3. We believe both approaches are viable, but will require additional engineering work.

Eye box. Although the 8 mm eye boxes of our prototype displays were suitable as monocular demonstrators, we require a larger eye box of 10–12 mm to achieve a practical stereo headset. This will require less angular selectivity in our holographic lenses. We will also need to introduce more degrees of freedom in our optical designs to correct optical aberrations over these larger eye boxes.

Display panels. Sourcing displays with higher pixel counts and pixel densities will be required to achieve human visual acuity in a dynamic display. We can also consider deliberately introducing pincushion distortion into our optical designs, which concentrates resolution at the center of the field of view where human visual acuity is the highest. The displayed image would also benefit from geometric, intensity uniformity, color uniformity, and color alignment calibration, which was not performed for our display prototypes.

Controlling leakage. We observed a moderate ghost image in the center of the FOV of our color prototype, which was most noticeable for content with a dark background. To suppress this ghost, we need to ensure that all optical surfaces in the design are anti-reflection coated. We may also improve performance by tuning the polarization control optics (i.e. quarter waveplates and polarizers) for the wavelengths of our lasers, rather than the whole visible spectrum.

Size and weight reduction. Our sunglasses-like prototype with an LCD panel (Section 4.2.2) had a display module that was 8.9 mm thick and weighted 17.8 g. If we were to reduce all substrate thicknesses to 0.5 mm, remove the inactive regions of the optics, and use a plastic rather than aluminum frame, we expect that we could reduce the thickness to 8.25 mm and the weight to 9.8 g with the same optical performance. If we removed the module frame entirely by mounting the optics directly into the glasses frame and switched to plastic substrates for all the optics, we expect that we could reduce weight to 6.6 g. Note that this is approximately the weight of a large "aviator" style sunglasses lens in 2 mm thick polycarbonate. However, the use of thin plastic substrates may pose challenges in rigidity and birefringence. We also acknowledge size reduction challenges when integrating light sources into the glasses, as current laser modules tend to be larger than commonly used LED sources.

Holographic lenses. Beyond reducing angular selectivity, we could improve our holographic lenses by better aligning the three recording lasers, ensuring beams are spatially uniform, and tuning recording parameters to improve diffraction efficiency. We could also use custom optics for recording that offer more degrees of freedom and compensate for recording material properties, like shrinkage.

Coherence and speckle. Our proposed designs benefit from the use of laser light sources with high temporal coherence to obtain the best resolution. To reduce the appearance of laser speckle in our prototypes, we used off-the-shelf laser despeckling units. However, to obtain the best form factor and performance, a custom despeckling unit could be employed in which the diffuser properties are matched to system parameters.

Varifocal display. We could apply various techniques to dynamically adjust the focus of the display to match the focal state of the viewer, such as mechanically moving one of the optical components, or using non-mechanical liquid crystal elements [Jamali et al. 2018]. However, we note that mechanical solutions may be an interesting solution in the proposed architectures since the required travel is very small and is estimated to be 50-150 microns per diopter of focus, depending on the display design. Thus, the total travel over the full range of accommodation could be < 1 mm. This limited travel range may open up new mechanical solutions like amplified piezoelectric actuation, although the required precision of the mechanical actuator would correspondingly increase.

System integration. Our prototypes were monoscopic and used external light sources and display drivers. A truly portable and practical display would integrate a pair of display modules, a computing platform, batteries, positional trackers, and all external components into a sunglasses-like frame.

6.2 Conclusion

Lightweight, high resolution, and sunglasses-like VR displays may be the key to enabling the next generation of demanding virtual reality applications that can be taken advantage of anywhere and for extended periods of time. We made progress towards this goal by proposing a new design space for virtual reality displays that combines polarization-based optical folding, holographic optics, and a host of supporting technologies to demonstrate full color display, sunglasses-like form factors, and high resolution across a series of hardware prototypes. Many practical challenges remain: we must achieve a full color display in a sunglasses-like form factor, obtain a larger viewing eye box, and work to suppress ghost images. In doing so, we hope to be one step closer to achieving ubiquitous and immersive computing platforms that increase productivity and bridge physical distance.

ACKNOWLEDGMENTS

We thank the team at Facebook Reality Labs and external partners for their advice and support on the project. Ryan Ebert, Dave Lindberg, Seth Moczydlowski, and Clinton Smith designed and fabricated the optics holder and frame for the sunglasses-like prototypes and provided mechanical component alignment and cutting tools. Ryan Ebert and Clinton Smith also suggested options for mechanical varifocal actuation. Junren Wang fabricated the polarization volume hologram with assistance from Stephen Choi and Babak Amirsolaimani. Babak also inspired the use of the polarization volume hologram in the design. Mengfei Wang and Lu Lu provided additional discussion and advice on liquid crystal optics. Bruce Cleary, Robert Birch, Alex Klement, and Savitre Balkissoon provided driving electronics and firmware for the display panels. Afsoon Jamali provided advice and support on polarization optics. Changwon Jang provided holographic element efficiency calculations that were used to guide the optical designs. Melissa Geng, Yang Zhao, Weichuan Gao, Brian Wheelwright, Jacques Gollier, and Barry Silverstein provided feedback, discussion, and advice on optics. Douglas Lanman suggested the use of a multimode optical fiber to carry a despeckled laser source and provided project guidance and writing advice.

REFERENCES

Takahisa Ando, Koji Yamasaki, Masaaki Okamoto, and Eiji Shimizu. 1998. Head-mounted display using a holographic optical element. In *Practical Holography XII*, Stephen A. Benton (Ed.), Vol. 3293. International Society for Optics and Photonics, SPIE, 183 – 189. https://doi.org/10.1117/12.303654

Tin M. Aye, Kevin Yu, Indra Tengara, Philipp W. Peppler, and Byron J. Pierce. 2001. Compact HMD optics based on multiplexed aberration-compensated holographic optical elements. In *Helmet- and Head-Mounted Displays VI*, Ronald J. Lewandowski, Loran A. Haworth, Henry J. Girolamo, and Clarence E. Rash (Eds.), Vol. 4361. International Society for Optics and Photonics, SPIE, 89 – 97. https://doi.org/10.1117/12.438010

M Blum, M Büeler, C Grätzel, J Giger, and M Aschwanden. 2012. Optotune focus tunable lenses and laser speckle reduction based on electroactive polymers. In *Moems and Miniaturized Systems Xi*, Vol. 8252. Intl. Society for Optics and Photonics, 825207.

Craig T Draper, Colton M Bigler, Micah S Mann, Kalluri Sarma, and Pierre-Alexandre Blanche. 2019. Holographic waveguide head-up display with 2-D pupil expansion and longitudinal image magnification. *Applied optics* 58, 5 (2019), A251–A257.

Ying Geng, Jacques Gollier, Brian Wheelwright, Fenglin Peng, Yusufu Sulai, Brant Lewis, Ning Chan, Wai Sze Tiffany Lam, Alexander Fix, Douglas Lanman, Yijing Fu, Alexander Sohn, Brett Bryars, Nelson Cardenas, Youngshik Yoon, and Scott McEldowney. 2018. Viewing optics for immersive near-eye displays: pupil swim/size and weight/stray light. In *Digital Optics for Immersive Displays*, Bernard C. Kress, Wolfgang Osten, and Hagen Stolle (Eds.), Vol. 10676. International Society for Optics and Photonics, SPIE, 19 – 35. https://doi.org/10.1117/12.2307671

J. W. Goodman. 1976. Some fundamental properties of speckle∗. *J. Opt. Soc. Am.* 66, 11 (Nov 1976), 1145–1150. https://doi.org/10.1364/JOSA.66.001145

Joseph W Goodman. 2005. Introduction to Fourier optics. *Introduction to Fourier optics, 3rd ed., by JW Goodman. Englewood, CO: Roberts & Co. Publishers, 2005* 1 (2005).

Hekun Huang and Hong Hua. 2018. High-performance integral-imaging-based light field augmented reality display using freeform optics. *Optics express* 26, 13 (2018), 17578–17590.

Roger Brian Huxford. 2004. Wide FOV head-mounted display using hybrid optics. In *Optical Design and Engineering*, Laurent Mazuray, Philip J. Rogers, and Rolf Wartmann (Eds.), Vol. 5249. International Society for Optics and Photonics, SPIE, 230 – 237. https://doi.org/10.1117/12.516541

Afsoon Jamali, Comrun Yousefzadeh, Colin McGinty, Douglas Bryant, and Philip Bos. 2018. LC lens systems to solve accommodation/convergence conflict in three-dimensional and virtual reality displays. *Optical Engineering* 57, 10 (2018), 1 – 8. https://doi.org/10.1117/1.OE.57.10.105101

Changwon Jang, Kiseung Bang, Gang Li, and Byoungho Lee. 2018. Holographic Near-Eye Display with Expanded Eye-Box. *ACM Trans. Graph.* 37, 6, Article Article 195 (Dec. 2018), 14 pages. https://doi.org/10.1145/3272127.3275069

Nam Kim, Yan-Ling Piao, and Hui-Ying Wu. 2017. Holographic optical elements and application. *Holographic Materials and Optical Systems. Rijeka, Croatia: InTech, Prolaz Marije Krucifikse Kozulić* (2017), 99–131.

Junji Kobashi, Hiroyuki Yoshida, and Masanori Ozaki. 2016. Planar optics with patterned chiral liquid crystals. *Nature Photonics* 10, 6 (2016), 389.

Herwig Kogelnik. 1969. Coupled Wave Theory for Thick Hologram Gratings. *Bell System Technical Journal* 48, 9 (1969), 2909–2947.

Douglas Lanman and David Luebke. 2013. Near-Eye Light Field Displays. *ACM Trans. Graph.* 32, 6, Article Article 220 (Nov. 2013), 10 pages. https://doi.org/10.1145/2508363.2508366

Joseph A. LaRussa and Arthur T. Gill. 1978. The Holographic Pancake Window TM. In *Visual Simulation and Image Realism I*, Leo Beiser (Ed.), Vol. 0162. International Society for Optics and Photonics, SPIE, 120 – 129. https://doi.org/10.1117/12.956898

Yun-Han Lee, Kun Yin, and Shin-Tson Wu. 2017. Reflective polarization volume gratings for high efficiency waveguide-coupling augmented reality displays. *Opt. Express* 25, 22 (Oct 2017), 27008–27014. https://doi.org/10.1364/OE.25.027008

Andrew Maimone, Andreas Georgiou, and Joel S. Kollin. 2017. Holographic Near-Eye Displays for Virtual and Augmented Reality. *ACM Trans. Graph.* 36, 4, Article Article 85 (July 2017), 16 pages. https://doi.org/10.1145/3072959.3073624

Andrew Maimone, Douglas Lanman, Kishore Rathinavel, Kurtis Keller, David Luebke, and Henry Fuchs. 2014. Pinlight Displays: Wide Field of View Augmented Reality Eyeglasses Using Defocused Point Light Sources. *ACM Trans. Graph.* 33, 4, Article Article 89 (July 2014), 11 pages. https://doi.org/10.1145/2601097.2601141

Bharathwaj Appan Narasimhan. 2018. Ultra-Compact pancake optics based on ThinEyes super-resolution technology for virtual reality headsets. In *Digital Optics for Immersive Displays*, Bernard C. Kress, Wolfgang Osten, and Hagen Stolle (Eds.), Vol. 10676. International Society for Optics and Photonics, SPIE, 359 – 366. https://doi.org/10.1117/12.2315688

Yi-Jun Wang, Shi-Hong Ouyang, Wei-Chung Chao, Jian-Gang Lu, and Han-Ping D Shieh. 2015. High directional backlight using an integrated light guide plate. *Optics Express* 23, 2 (2015), 1567–1575.

Timothy L. Wong, Zhisheng Yun, Gregg Ambur, and Jo Etter. 2017. Folded optics with birefringent reflective polarizers. In *Digital Optical Technologies 2017*, Bernard C. Kress and Peter Schelkens (Eds.), Vol. 10335. International Society for Optics and Photonics, SPIE, 84 – 90. https://doi.org/10.1117/12.2270266